



# FUNDAMENTALS OF BRITTLE FAILURE AT THE ATOMIC SCALE

Laurent Brochard, Sabri Souguir, Karam Sab

## ► To cite this version:

Laurent Brochard, Sabri Souguir, Karam Sab. FUNDAMENTALS OF BRITTLE FAILURE AT THE ATOMIC SCALE. 10th International Conference on Fracture Mechanics of Concrete and Concrete Structures, Jun 2019, Bayonne, France. <10.21012/FC10.235517>. <hal-03170502>

**HAL Id: hal-03170502**

**<https://hal.science/hal-03170502v1>**

Submitted on 16 Mar 2021

**HAL** is a multi-disciplinary open access archive for the deposit and dissemination of scientific research documents, whether they are published or not. The documents may come from teaching and research institutions in France or abroad, or from public or private research centers.

L'archive ouverte pluridisciplinaire **HAL**, est destinée au dépôt et à la diffusion de documents scientifiques de niveau recherche, publiés ou non, émanant des établissements d'enseignement et de recherche français ou étrangers, des laboratoires publics ou privés.



HAL Authorization

# FUNDAMENTALS OF BRITTLE FAILURE AT THE ATOMIC SCALE

LAURENT BROCHARD\*, SABRI SOUGUIR\* AND KARAM SAB\*

\*Laboratoire Navier, UMR 8205, Ecole des Ponts, IFSTTAR, CNRS  
6 & 8 avenue Blaise Pascal, 77455 Marne-la-Valle Champs-sur-Marne, France  
e-mail: laurent.brochard@enpc.fr

**Key words:** Crack initiation, Stress Concentration, Graphene, Instability, Scaling Law, Atomistic Simulation

**Abstract.** In this work, we investigate the elementary processes of brittle failure initiation with molecular simulation techniques. Failure initiation theories aim at bridging the gap between energy-driven failure at high stress concentrations and stress-driven failure in absence of stress concentration, and thus capturing the transition at moderate stress concentrations and associated scale effects. We study graphene, which is one of the few materials with a sufficiently small characteristic length (ratio between toughness and strength) to be addressed by molecular simulations. We also consider a toy model that proves helpful for physical interpretations. Performing molecular simulations of pre-cracked graphene, we found that its failure behavior can overcome both strength and toughness in situations of very high or low stress concentrations, respectively; which is consistent with one particular theory, namely Finite Fracture Mechanics (FFM), which considers failure initiation as the nucleation of a crack over a finite length. Details of the atomic mechanisms of failure are investigated in the athermal limit (0K). In this limit, failure initiates as an instability (negative eigenvalue of the Hessian matrix), irrespective of the stress concentration. However, the atomic mechanisms of failure and their degeneracy (eigenvector of the negative eigenvalue) strongly depend on stress concentration and points to the nucleation of a deformation band whose length decreases with stress concentration. This atomic description is quite similar to FFM theory. At finite temperature, failure is no more deterministic because of thermal agitation. An extensive study to characterize the effects of temperature, loading rate and system size leads to the formulation of a universal scaling law of strength and toughness which extends existing theory (Zhurkov) to size effects. Interestingly, the scalings of stress-driven failure (strength) and of energy-driven failure (toughness) differ only regarding the scaling in size, which relates to the effect of stress concentration on degeneracy identified in the athermal limit.

## 1 INTRODUCTION

Brittle failure is a long standing issue in mechanical engineering, but the physics of its initiation is still debated in the scientific community. Two cases are well established. The case of cracked bodies is well described by fracture mechanics which predicts failure when the energy released by the propagation of the crack exceeds a critical value, or equivalently when

the stress intensity at the tip exceeds the toughness ( $K_c$ ). In contrast, in the absence of stress concentration, the failure of a material follows a stress criterion instead of an energy criterion: failure occurs when stress exceeds a critical value known as strength  $\sigma_c$ . Strength and toughness are independent properties with different units, and their ratio points to a characteristic length  $l_c = \left(\frac{K_c}{\sigma_c}\right)^2$  intrinsic to the mate-

rial, often referred to as the size of the process zone. This characteristic length is the source of size effects in brittle failure and quantifies the scale at which one observes a transition from energy driven failure to stress driven failure. Brittle failure initiation theories aim at addressing this transition with generalized failure criteria that apply irrespective of the stress concentration while being consistent with energy- and stress-driven failures in the two aforementioned cases. Let us mention the Phase Field approaches [1], the Cohesive Zone Models (CZM) [2], the non local theories [3], and the Finite Fracture Mechanics (FFM) [4]. All these theories have been formulated from a macroscopic point of view based on postulated underlying mechanisms. In this work, we use molecular simulation techniques to investigate the elementary mechanisms of brittle failure at the scale of the characteristic length  $l_c$ . Doing so we aim to understand what are the elementary differences between energy- and stress-driven failures, and try to identify a general description of failure that would encompass both situations. Ultimately, such a description could help formulate a generalized macroscopic criterion for brittle failure.

This paper is organized as follows : section 2 presents the materials and simulation methods, section 3 investigates the size effects and stress concentration effects at the atomic scale, section 4 investigates the elementary mechanisms of failure initiation in the athermal limit (0K), and section 5 investigates the effect of finite temperature.

## 2 SIMULATION METHODS

For the vast majority of materials, the characteristic length  $l_c$  is inaccessible to classical molecular simulation techniques which are limited to systems of a few tens of nanometers. Graphene, though, exhibits a characteristic length of about 1 nm, which makes it an ideal candidate for a systematic study of failure initiation by molecular simulation. Graphene is a crystalline material made of carbons arranged in a honeycomb lattice (Fig. 1), well-known for its

exceptional electronic, thermal, and mechanical properties. It has an extremely high strength (130 GPa , [5]), but a moderate toughness ( $4 \text{ MPa} \cdot \sqrt{\text{m}}$  [6]) so that its failure behavior is extremely brittle with a process zone 4 to 5 atoms large only. In addition, we study a toy model: a triangular lattice with pair interactions between closest neighbors only (Fig. 1). The simplicity of the toy model makes it possible to confront easily molecular simulation results and theory, which proves useful for the interpretation of the failure mechanisms. This toy model is designed to exhibit a very brittle behavior with a characteristic length comparable to the size of a single bond.

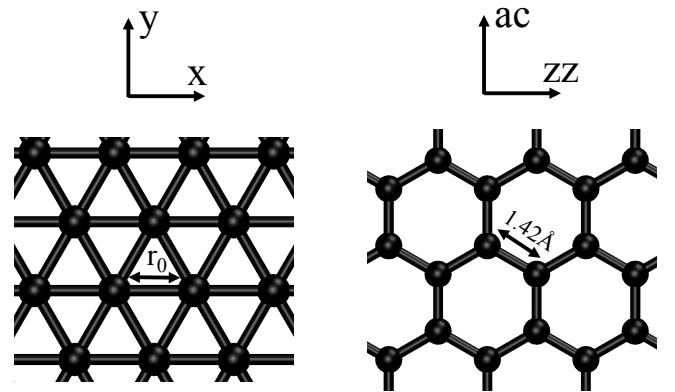


Figure 1: The two materials investigated : a toy model of triangular lattice (left), and graphene (right).

In this work, we study brittle failure with classical molecular simulations. Classical molecular simulations rely on empirical interatomic potentials, in contrast with 'ab-initio' molecular simulations which rely on first principles only. For the study of mechanical failure, it is necessary to consider reactive empirical potentials, that is potentials that have the ability to capture bond breaking and formation. A reactive potential adapted to graphene is the REactive Bond Order (REBO) potential [7]. For the toy model, we use a harmonic potential between nearest neighbor. A cutoff is applied which corresponds to a bond breaking. For the stability analysis (section 4), we use a smooth cutoff to ensure continuity of the potential and its derivatives. Molecular simulations are all per-

formed with periodic boundary conditions using the minimum image convention, and mechanical loading is prescribed by controlling the size of the periodic box. Simulations at finite temperatures (sections 3, 5) are performed by molecular dynamics, whereas simulations in the athermal limit (0K) are performed by energy minimization. All simulations are performed with LAMMPS (<http://lammps.sandia.gov>, [8]). See [9–11] for more details regarding the set up of the molecular simulations.

### 3 TRANSITION BETWEEN ENERGY AND STRESS CRITERIA

Size effects are expected when the size of a structure approaches the characteristic size  $l_c$ . In this regime, one expects a transition from energy-driven failure to stress driven failure. We investigate this transition by considering the failure of pre-cracked systems (Fig. 2). According to fracture mechanics the propagation of the crack occurs when the remote loading stress reaches :  $\Sigma_{cr} = \frac{K_c}{\sqrt{\pi a C(\frac{2a}{L})}}$ , where  $a$  is the crack half length and  $L$  the size of the periodic box. The factor  $C(2a/L)$  is a correction to account for the periodicity of the system, in particular one recovers the usual case of a finite crack in an infinite body ( $C = 1$ ) in the limit  $2a/L \rightarrow 0$ . This energy-driven failure criterion is displayed in red in Fig. 2. When the size of the crack or the distance between periodic crack tips approaches  $l_c$  (i.e., very small or very long cracks), one expects a deviation from energy-driven failure. The limit of stress-driven failure is given by the case depicted in blue in Fig. 2, for which there is no more stress concentration. Stress-driven failure is expected when the remote loading stress reaches  $\Sigma_{cr} = \sigma_c(L - 2a)$  (stress reaches strength). The relative position between energy-driven failure and stress-driven failure depends on the ratio between the size  $L$  of the periodic system and the characteristic length  $l_c$ . The situation of interest regarding size effect is when the relative position of the two criteria change in function of the crack length, which requires  $L/(2l_c) > 1.96$  (Fig. 2).

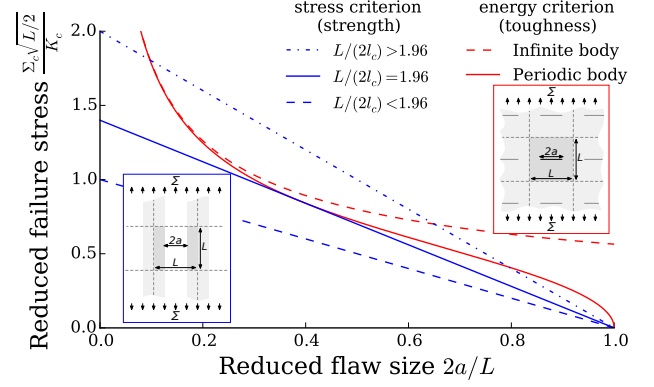


Figure 2: **Relative position of of stress- and energy-driven failure criteria for a periodic flawed material in function of the flaw and system size.** The situation of interest for the study of size effects is when the relative positions of the criteria alternate which occurs if the system is large enough compared to the characteristic length  $l_c$ .

Applying this strategy to graphene, we perform a series of molecular simulations of pre-cracked systems with  $L = 10$  nm and various length  $2a$  of the initial crack. The critical stress at failure are computed and confronted to the energy- and stress-driven failure criteria in Fig. 3. On the same Figure, we display the energy and stress criteria. For the energy criterion, toughness is estimated from the failure of a 20 nm pre-cracked system, with crack sizes limited to the domain of validity of fracture mechanics (i.e.,  $2a$  and  $L - 2a$  significantly larger than  $l_c$ ). For the stress criterion, the strength is estimated from the failure of a 10 nm flawless system. In Figure 3, we observe a clear transition from the energy criterion to the stress criterion at small crack lengths ( $2a \rightarrow 0$ ). In contrast, at large crack lengths ( $2a \rightarrow L$ ) failure seems to follow the energy and the stress criterion is overcome. The failure at large crack lengths is surprising since most initiation theories would generally predict a failure bounded by the intersection between energy and stress criteria, i.e., would not allow to overcome strength. Interestingly, this is allowed in the theory of Finite Fracture Mechanics (FFM) [4]. According to FFM, failure initiates with the nucleation of a crack of finite length if: 1) stress exceeds strength over this finite length, and 2) the in-

cremental energy released exceeds the energy release rate times the nucleation length. This mixed criterion predicts that one can overcome strength in particular cases for which the incremental energy release is not sufficient to satisfy the second condition. This is indeed the case for the systems of Figure 3 at large crack lengths: in such systems, the tips of periodic cracks are very close so that stresses are highly concentrated (condition on stress easily met), but the systems are very compliant so that little mechanical energy is available (condition on energy release is hard to satisfy). In Figure 3, we compute the failure predicted by FFM (in blue). FFM captures reasonably well the failure behavior of pre-cracked graphene over the full range of crack lengths. In particular, it captures the transition from energy- to stress-driven failure at small crack lengths. And, most interestingly, it overcomes the strength at large crack lengths.

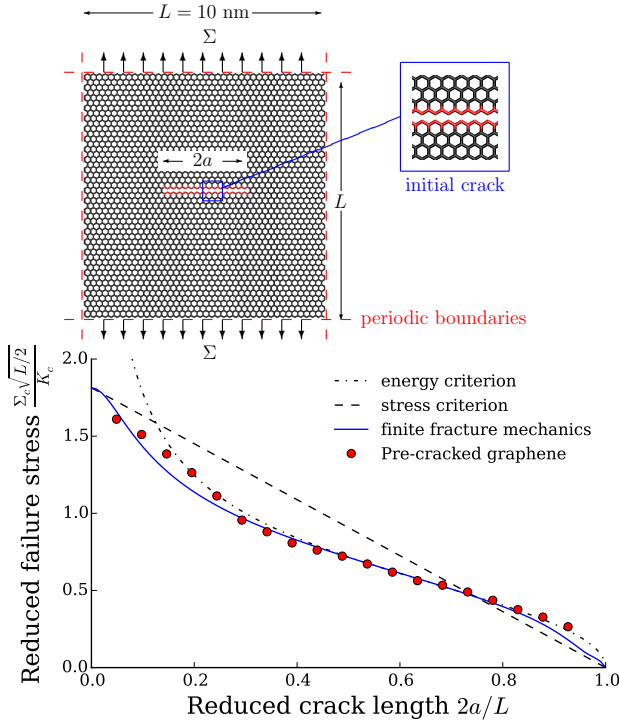


Figure 3: Remote stress at failure for 10 nm pre-cracked periodic graphene systems in function of the crack length. Failure appears to be limited by strength at small crack lengths and by energy release at large crack lengths, which is reasonably captured by the initiation theory of FFM.

An other way to address the transition between energy- and stress-driven failures is to consider flaws of varying stress concentration, e.g., notch or holes. We consider 20 nm periodic systems with elliptic holes (Fig. 4) and we compute how failure stress changes with the aspect ratio of the hole (the length of the hole is constant :  $2a = L/2$ , and only the width  $2b$  is varied). As expected, one observes a transition from the energy-driven failure at small aspect ratios (limit of a crack) to stress-driven failure at large aspect ratios. Applying FFM to these systems provides predictions consistent with the molecular simulation results.

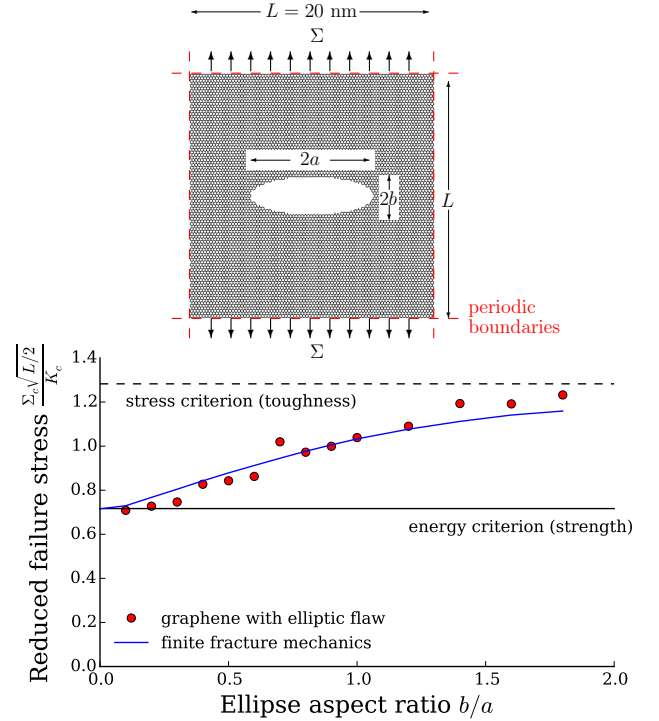


Figure 4: Remote stress at failure for 20 nm periodic graphene system with elliptic flaws in function of the aspect ratio of the flaw. The continuous transition from energy-driven failure at small aspect ratio to stress-driven failure at large aspect ratio is well captured by FFM.

The results of Figures 3 and 4 suggest that the mixed criterion proposed by FFM is an appropriate description of failure initiation. This is but a simple comparison, and we have not taken advantage of the large atomic scale data offered by molecular simulation. This is the purpose of the next section.

#### 4 ATHERMAL LIMIT: FAILURE INITIATION AS AN INSTABILITY

To investigate the elementary mechanisms of failure initiation, we first consider the athermal limit, i.e., the limit of the system at 0K. At non zero temperature, description of atomic systems is necessarily probabilistic because of thermal agitation, and each macroscopic state is associated with a multitude of atomic configurations, following Boltzmann statistics. Considering the athermal limit reduces significantly the complexity of the atomic description, since the problem becomes deterministic: a macroscopic state is associated to a single atomic configuration (that of minimum energy). All atomic momenta are zero, and the atomic structure corresponds to the static equilibrium of the system. In this limit an irreversible process such as mechanical failure is expected to occur when the system reaches a saddle point of the energy landscape and escapes from the energy well corresponding to the elastic domain. Said otherwise, failure is expected as an instability at the atomic scale. Therefore, a way to investigate the mechanisms of failure in the athermal limit consists in characterizing the modes of instability of the atomic system. An instability occurs when one of the eigenvalues of the Hessian matrix of the energy becomes negative. The associated eigenvectors provides the movement of the atoms at the point of instability, which we refer to as mode of failure.

Following this strategy, we perform athermal simulations of failure of periodic graphene systems with and without crack, and we compute the smallest eigenvalue of the Hessian matrix (Fig. 5). As expected, we observe failure precisely when the smallest eigenvalue becomes negative. The corresponding eigenvectors (modes of failure) are displayed in Figure 5. Interestingly, the mode of failure is very localized for the pre-cracked system, but delocalized for the flawless system. The mode of failure in absence of stress concentration is the nucleation of a deformation band that spans over the entire system, whereas the nucleation is limited to the vicinity of the crack tip for the flawed systems.

The mode of failure of the flawless system is non obvious since the evolution at failure could bifurcate to many different configurations such as the breakage of a single bond, or a pair of bonds. Instead, the mode of failure of the pre-cracked system is quite intuitive since one expects only few possible bifurcations at failure all corresponding to bond breakage close to the crack tips. Therefore, the elementary mechanism of brittle failure in the athermal limit is an instability that leads to the nucleation of a crack over a length that strongly depends on the stress concentration. Interestingly, FFM theory also predicts a nucleation over the entire length of the system in absence of stress concentration and a nucleation over a length of the order of the characteristic length  $l_c$  for high stress concentrations ( $l_c = 6.8\text{\AA}$  for the molecular model of graphene). Here, the nucleation at the crack tip seems a little smaller than  $l_c$ , but a minimum nucleation length of one or a few bond lengths makes sense from an atomic perspective.

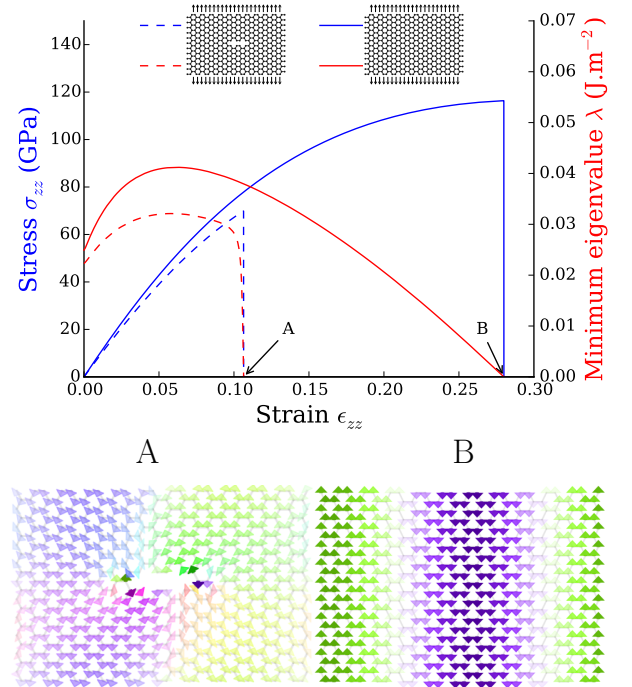


Figure 5: In the athermal limit, failure of graphene is an instability at the atomic scale (negative eigenvalue of the Hessian matrix), irrespective of the stress concentration. However, the mode of failure (eigenvector) strongly depends on the stress concentration.



We perform a similar analysis for the failure of the toy model in the athermal limit (Fig. 6). Again, failure corresponds to an instability at the atomic scale, irrespective of the stress concentration; but stress concentration strongly affects the mode of failure. It is worth noting that, at least for flawless systems, the orientation of failure initiation is an interplay between the loading and the crystal orientation (vertical bands in Fig. 5, oblique in Fig. 6). This peculiarity has probably to do with the orientation dependence of strength which is not addressed in usual FFM formulations.

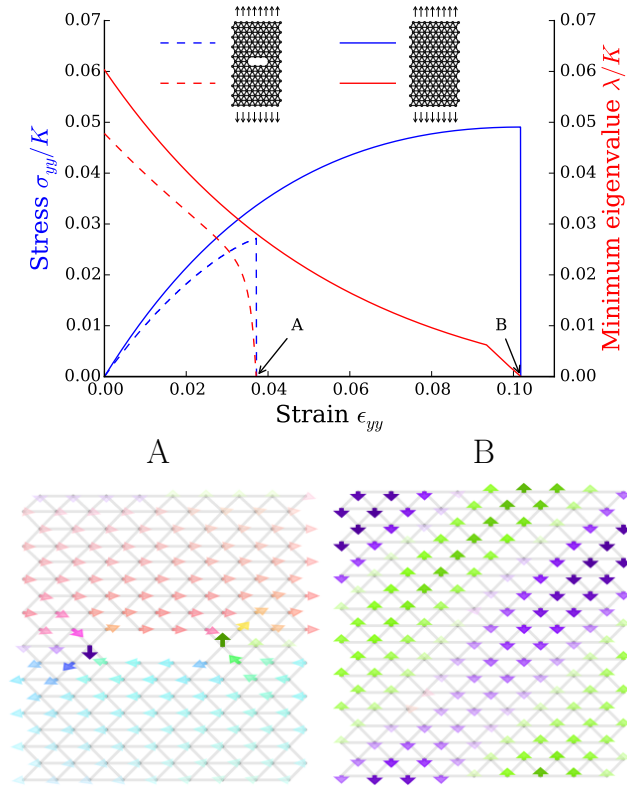


Figure 6: **Failure of the toy model in the athermal limit.**

An other important effect of stress concentration is the degeneracy of the mode of failure. In the athermal limit, degeneracy does not affect the stress at failure. But, it is of great importance for failure at finite temperatures (next section). Computing the spectrum of the Hessian matrix, one readily observes that the smallest eigenvalue is highly degenerated in absence of stress concentration, but very little degenerated

in presence of a crack. Of course, degeneracy is expected to be closely related to the physical symmetries of the system, which is broken by the presence of the crack. Yet how this degeneracy scales with the size of the system (number of atoms  $N$ ) is absolutely non obvious (Tab. 1). The scaling of degeneracy is of the form  $\alpha N^\beta$  with  $\alpha$  and  $\beta$  quantities that depend on both the material and the loading. For the cases studied in this work, the exponent  $\beta$  is either 0.5 or 1 (for homothetic change of size), which could be explained by degeneracy related to a number of lines or diagonals (0.5) or to the number of bonds 1, but the origin of the scaling remains unclear. In contrast, there is no degeneracy in presence of a crack and this holds irrespective of the size of the system. In practice, degeneracy can be interpreted as the number of different transition paths (saddle points) of same minimum energy that lead to instability, i.e., the number of possible atomic mechanisms triggering failure. Although, we investigate here only the two extreme cases (no stress concentration and high stress concentration), one can readily anticipate the impact of stress concentration: as soon as a little stress concentration is introduced, degeneracy is immediately removed and the transition paths to failure exhibit different energies. Only the path of smallest energy is reached in the athermal limit, but at finite temperature, competition between the different paths is significant if the differences between transition path energies are of the order of the thermal agitation energy. As stress concentration is increased, the difference of energies are exacerbated and the system is expected to fail via the transition path of minimum energy only.

Table 1: Scaling of the degeneracy of the mode of failure obtained by repeating the athermal stability analysis for systems of different sizes (homothetic systems).

system	loading direction	degeneracy
flawless	ac	$0.3N^{0.5}$
graphene	zz	$0.2N$
flawless	x	$1.3N^{0.5}$
toy model	y	$N$

## 5 FAILURE INITIATION AT FINITE TEMPERATURE

At finite temperature, thermal agitation requires to adopt a statistical description of brittle failure. Each macroscopic state corresponds to a large number of atomic configurations with probabilities following Boltzmann statistics. Accordingly, a transition state leading to failure can be reached with a probability proportional to  $\exp(-\frac{\Delta E}{kT})$ , where  $\Delta E$  is the energy to overcome to reach the transition state,  $k$  is Boltzmann constant and  $T$  is the temperature. From a time evolution perspective, probability of occurrence of a transition state can be viewed as the inverse of the average time needed to reach this transition state. Therefore, at finite temperature, one expects average failure stress to depend on temperature and loading time (or equivalently loading rate). Moreover, as discussed at the end of the previous section, the number of transition states depends on the system size. The probability of failure is the cumulative probability of all transition states. So, one can also expect that failure depends on the system size. Accordingly, we perform a systematic study of brittle failure properties (strength and toughness) at finite temperature by investigating the combined effects of i) temperature, ii) loading rate, and iii) system size. Because of the high computational cost, this systematic study is limited to the toy model, whereas for graphene we investigated the effect of temperature only. Strength was estimated directly from the failure of flawless systems, whereas toughness was estimated from the failure of pre-cracked systems with varying initial crack sizes following the methodology described in section 3. Special attention is paid to consider crack sizes that avoid any size effects. The results for graphene are presented in Fig. 7 and for the toy model in Fig. 8.

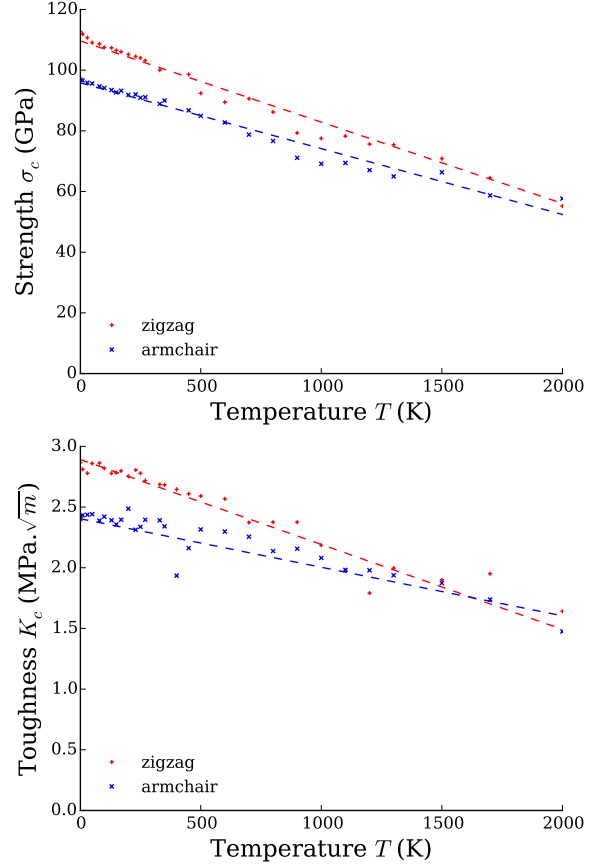


Figure 7: **Strength and toughness of graphene as a function of temperature.**

We observe that strength and toughness follow very similar scalings ( $\propto (1 - T/T_0)$  for graphene, and  $\propto (1 - \sqrt{T/T_0})$  for the toy model). This points to a similar form of the energy barrier  $\Delta E$  in function of the remote loading, irrespective of the stress concentration. This can be proven formally for the toy model, since atomic interactions are all linear (see demonstration in [10]). The energy barrier  $\Delta E \propto \left(1 - \frac{\Sigma}{\Sigma_0}\right)^2$  relates to the remote stress (with  $\Sigma_0$  the remote stress at failure at 0K), and remote stress quantifies both strength and toughness for flawless and pre-cracked systems, respectively. Therefore, energy- and stress-driven failures are not only of similar origin at 0K (atomic instability), but their evolution with temperature remains analogous. Interestingly, this observation holds for a realistic material like graphene, which is non obvious a priori (no



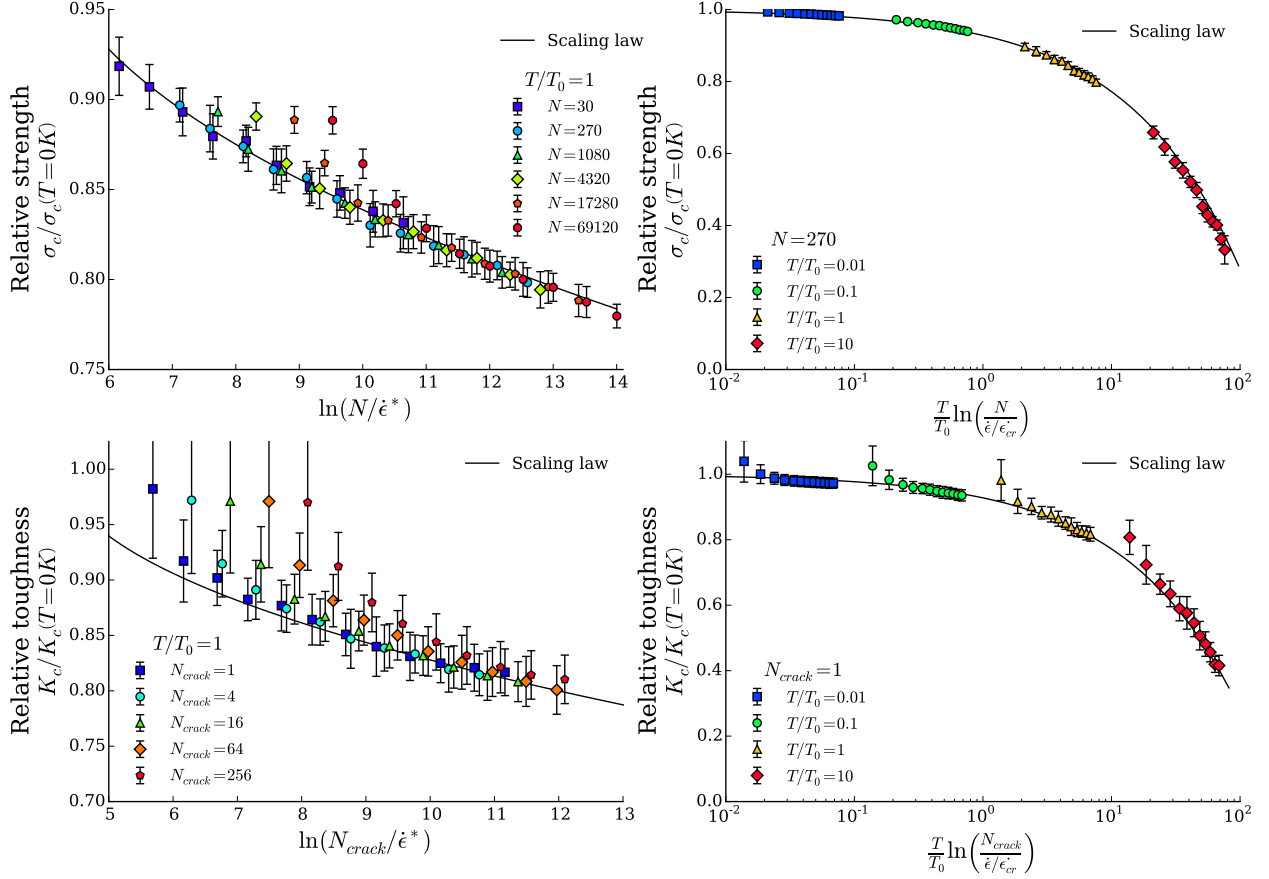


Figure 8: **Detailed scaling of strength and toughness of the toy model in function of temperature, loading rate and system size.** Strength and toughness follow identical scalings except for the system size: strength scales with the number of atoms, whereas toughness scales with the number of cracks.

formal demonstration is possible with a complex potential like REBO). The difference in scaling between graphene and the toy model is reminiscent of the atomic interactions. Numerical estimation of the transition path energy can be achieved for graphene, and leads to an energy barrier different from that of the toy model:  $\Delta E \propto 1 - \frac{\Sigma}{\Sigma_0}$  [10]. Interestingly, a majority of brittle materials exhibit a linear scaling of strength with temperature like graphene, which is known as Zhurkov's law [12]. The non-physical truncation of the linear interactions in the toy model is responsible for the peculiarity of its scaling, whereas real inter-atomic interactions are smooth at failure.

Investigating the effects of loading rate ( $\dot{\epsilon}$ ) for the toy model (Fig. 8), we could identify a temperature-rate equivalency, with a scaling of the form  $-T \ln(\dot{\epsilon})$ . Again, the same scal-

ing is observed for both strength and toughness, which means that this temperature-rate equivalence holds irrespective of stress concentration. This equivalence is easily understood from Boltzmann probability. Under the ergodic hypothesis, the probability to reach a transition state to failure ( $\propto \exp\left(-\frac{\Delta E(\Sigma)}{kT}\right)$ ) quantifies the inverse of the characteristic time to failure. Equivalently, the probability of failure over a given time scale is inversely proportional to the loading rate. Therefore, the loading at failure verifies  $\Delta E(\Sigma) = \frac{T}{T_0} \ln\left(\frac{\dot{\epsilon}_0}{\dot{\epsilon}}\right)$ . Zhurkov's law also addresses time effects, through the characteristic time at failure. The rate-temperature equivalence we identify here is precisely Zhurkov's law, by considering loading rate scaling as the inverse of the scaling of time at failure.

A last effect, which is not addressed in

Zhurkov's law, is the effect of system size. In contrast with the effects of temperature and loading rate, the effect of system size on the strength and toughness of the toy model is radically different (Fig. 8): strength decreases with the number of atoms, but toughness is independent of the number of atoms. Instead, by considering pre-cracked systems with multiple identical cracks within the periodic simulation box (Fig. 9), we identify that toughness scales with the number of cracks instead of the number of atoms. Indeed, the presence of multiple cracks within the periodic box offers more transition paths to failure (periodic replicas of cracks do not offer additional transition paths since their behavior is identical to that of the original cracks). The number of transition states  $N_{TS}$  to failure controls the effects of system size. Indeed, the total probability of failure is the cumulative probability of all available transition states. If all transition states are identical (degenerate energy barrier  $\Delta E$ ), the probability of failure is of the form:  $\propto N_{TS} \exp(-\frac{\Delta E}{kT})$ , so that one gets a universal temperature-rate-size equivalence of the form  $\frac{T}{T_0} \ln\left(\frac{N_{TS}}{\dot{\epsilon}/\dot{\epsilon}_0}\right)$ . As we discussed in the athermal limit, the transition states are indeed degenerated and the degeneracy scales as a power of the number of atoms ( $N_{TS} \propto N$  for the toy model loaded in y, as is the case here). Similarly, one expects the different paths to failure to be degenerated in the case of pre-cracked systems with multiple cracks (Fig. 9), with a degeneracy that scales as the number of cracks, and independent of the number of atoms:  $N_{TS} \propto N_{crack}$ . These degeneracies are consistent with the size scalings of strength and toughness of the toy model (Fig. 8). This scaling with size allows us to formulate a generalized version of Zhurkov's law, which is of practical interest as soon as one is concerned with many time or length scales:

$$\frac{\Sigma}{\sigma_0} = 1 - \left( \frac{T}{T_0} \ln \left( \frac{N_{TS}}{\dot{\epsilon}/\dot{\epsilon}_0} \right) \right)^\gamma \quad (1)$$

where  $\gamma$  is  $1/2$  for the toy model, but is expected to be 1 for a majority of materials.

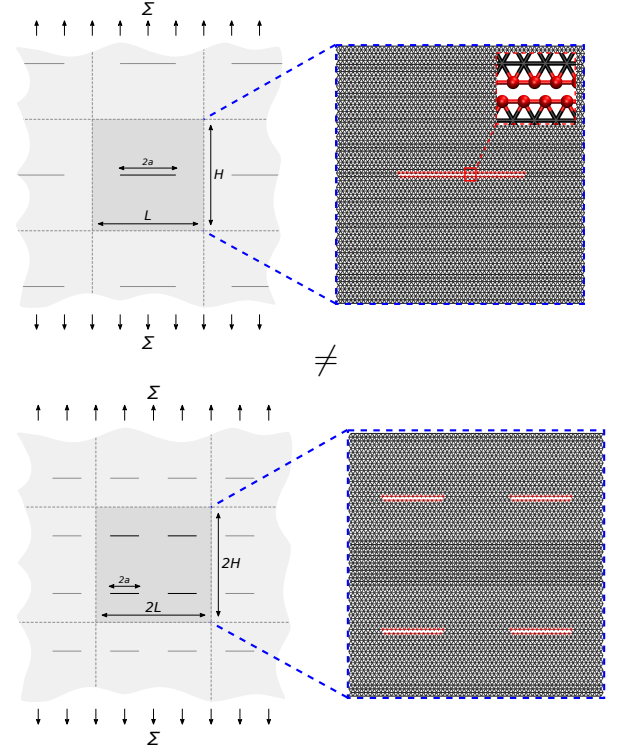


Figure 9: These two systems are not statistically equivalent regarding failure. When the periodic cell contains a single crack, failure initiates at all the periodic replicas at the same time. Whereas, when the periodic cell contains multiple cracks, multiple transition paths to failure are available each corresponding to the advance of one of the cracks only (and its periodic replicas). Therefore, because of the statistical nature of failure at finite temperature, brittle failure of pre-cracked systems is expected to depend on the number of cracks in the periodic cell.

## 6 CONCLUSIONS

In this work, we investigated the elementary physics of brittle failure at the atomic scale, and more precisely the transition from energy-driven failure to stress-driven failure. We study the case of graphene because of its highly brittle behavior which makes it possible to capture this transition at a scale compatible with the computational limits of molecular simulation. We find that failure initiation in graphene is well captured by FFM. According to FFM, failure initiates by the nucleation of a crack over a length that vary depending on the stress concentration. Looking at the detailed atomic mechanisms of failure in the athermal limit, we

find that failure always initiates as an atomic instability, and the associated mode of instability strongly depends on stress concentration. One observes the nucleation of deformation bands whose length increases with stress concentration, which, again, is quite consistent with FFM description of failure initiation. The mode of instability exhibit a strong degeneracy in absence of stress concentration (scaling with the number of atoms), but no degeneracy under stress concentration. At finite temperatures, a statistical description of failure is necessary to account for thermal agitation. The configuration of instability in the athermal limit are replaced by transition states whose probabilities of occurrence are given by Boltzmann statistics. Following the ergodic hypothesis, this probability relates to a characteristic time to trigger failure. Moreover, degeneracy of the instability mode in the athermal limit suggests that transition states are also potentially degenerated which is expected to induce effects of system size at finite temperature. Through an extensive study of strength and toughness at finite temperature, we identify a general scaling law of brittle failure, that extends Zhurkov's law to size effects and proves applicable to both stress-driven failure (strength) and energy-driven failure (toughness). Strength and toughness scalings differ only regarding the effects of system size: scaling with the number of atoms for strength, and with the number of cracks for toughness. This difference is reminiscent of the degeneracy of instability modes in the athermal limit.

The results of this work tend to support a description of brittle failure initiation as the unstable nucleation of a flaw, the size of which strongly depends on the degree of stress concentration. Such a description is similar to FFM theory. As expected from this theory, the nucleation length decreases with stress concentration. However, additional investigations are needed for a quantitative assessment of the mixed energy-stress criterion of FFM. Also, the current study is limited to a pristine material, and accounting for defects in real materials is a necessary step for future research.

## ACKNOWLEDGEMENTS

We gratefully acknowledge funding from the Labex MMCD provided by the national program Investments for the Future of the French National Research Agency (ANR-11-LABX-022-01)

## REFERENCES

- [1] C. Miehe, F. Welschinger, and M. Hofacker. Thermodynamically consistent phase-field models of fracture: Variational principles and multi-field FE implementations. *International Journal for Numerical Methods in Engineering*, 83(10):1273–1311, sep 2010.
- [2] D.S. Dugdale. Yielding of steel sheets containing slits. *Journal of the Mechanics and Physics of Solids*, 8(2):100–104, 1960.
- [3] V.V. Novozhilov. On a necessary and sufficient criterion for brittle strength. *Journal of Applied Mathematics and Mechanics*, 33(2):201–210, jan 1969.
- [4] Dominique Leguillon. Strength or toughness? A criterion for crack onset at a notch. *European Journal of Mechanics, A/Solids*, 21(1):61–72, 2002.
- [5] Changgu Lee, Xiaoding Wei, Jeffrey W Kysar, and James Hone. Measurement of the Elastic Properties and Intrinsic Strength of Monolayer Graphene. *Science*, 321(5887):385–388, jul 2008.
- [6] Peng Zhang, Lulu Ma, Feifei Fan, Zhi Zeng, Cheng Peng, Phillip E. Loya, Zheng Liu, Yongji Gong, Jiangnan Zhang, Xingxiang Zhang, Pulickel M. Ajayan, Ting Zhu, and Jun Lou. Fracture toughness of graphene. *Nature Communications*, 5(1):3782, dec 2014.
- [7] Donald W. Brenner. Empirical potential for hydrocarbons for use in simulating the chemical vapor deposition of diamond

- films. *Physical Review B*, 42(15):9458–9471, nov 1990.
- [8] Steve Plimpton. Fast Parallel Algorithms for Short-Range Molecular Dynamics. *Journal of Computational Physics*, 117(1):1–19, mar 1995.
- [9] Laurent Brochard, Ignacio G. Tejada, and Karam Sab. From yield to fracture, failure initiation captured by molecular simulation. *Journal of the Mechanics and Physics of Solids*, 95:632–646, oct 2016.
- [10] Laurent Brochard, Sabri Souguir, and Karam Sab. Scaling of brittle failure: strength versus toughness. *International Journal of Fracture*, 210(1-2):153–166, mar 2018.
- [11] Souguir et al. Atomistic processes of brittle failure initiation in the athermal limit. *in preparation*, 2019.
- [12] S. N. Zhurkov. Kinetic concept of the strength of solids. *International Journal of Fracture*, 26(4):295–307, dec 1984.